STEM CELLS AND DEVELOPMENT
Volume 28, Number 10, 2019
Mary Ann Liebert, Inc.
DOI: 10.1089/scd.2018.0230

Dentinogenesis and Tooth-Alveolar Bone Complex Defects in *BMP9/GDF2* Knockout Mice

Xia Huang,[1,2] Feilong Wang,[2,3] Chen Zhao,[4] Sheng Yang,[1,5] Qianyu Cheng,[1,2] Yingying Tang,[1,2] Fugui Zhang,[1] Yan Zhang,[1] Wenping Luo,[1] Chao Wang,[1] Pengfei Zhou,[1] Stephanie Kim,[6] Guowei Zuo,[7] Ning Hu,[4] Ruidong Li,[8] Tong-chuan He,[1,6] and Hongmei Zhang[1,2]

Tooth development is regulated by sequential and reciprocal epithelium-mesenchymal interactions and their related molecular signaling pathways, such as bone morphogenetic proteins (BMPs). Among the 14 types of BMPs, BMP9 (also known as growth differentiation factor 2) is one of the most potent BMPs to induce osteogenic differentiation of mesenchymal stem cells. The purpose of this study was to examine potential roles of BMP9 signaling in tooth development. First, we detected the expression pattern of BMP9 in tooth germ during postnatal tooth development, and we found that BMP9 was widely expressed in odontoblasts, ameloblasts, dental pulp cells, and osteoblasts in alveolar bones. Then, we established a *BMP9*-KO mouse model. Gross morphological examination revealed that the tooth cusps of *BMP9*-KO mice were significantly abraded with shorter roots. Micro-computed tomography and three-dimensional reconstruction analysis indicated that the first molars of the *BMP9*-KO mice exhibited a reduced thickness dentin, enlarged pulp canals, and shortened roots, resembling the phenotypes of the common hereditary dental disease dentinogenesis imperfecta. Further, the alveolar bone of the *BMP9*-KO mutants was found to be shorter and had a decreased mineral density and trabecular thickness and bone volume fraction compared with that of the wild-type control. Mechanistically, we demonstrated that both dentin sialophosphoprotein and dentin matrix protein 1 were induced in dental stem cells by BMP9, whereas their expression was reduced when BMP9 was silenced. Further studies are required to determine whether loss of or decreased BMP9 expression is clinically associated with dentinogenesis imperfecta. Collectively, our results strongly suggest that BMP9 may play an important role in regulating dentinogenesis and tooth development. Further research is recommended into the therapeutic uses of BMP9 to regenerate traumatized and diseased tissues and for the bioengineering of replacement teeth.

Keywords: bone morphogenetic protein 9, dentinogenesis, tooth development, dental stem cells, odontoblastic differentiation, dentinogenesis imperfecta

Introduction

Tooth development is regulated by sequential and reciprocal epithelium-mesenchymal interactions and their related molecular signaling [1,2]. Tooth formation is a complex process that involves many types of dental stem cells and growth and transcriptional factors, in which multiple signaling pathways converge to regulate enamel and dentin formation [3–10]. Enamel formation results from the dental inner enamel epithelium cells differentiating into ameloblasts and dentin originates from mesenchyme that differentiate into odontoblasts in a spatiotemporal pattern

[1]Chongqing Key Laboratory for Oral Diseases and Biomedical Sciences, The Affiliated Hospital of Stomatology, Chongqing Medical University, Chongqing, China.
[2]Department of Pediatric Dentistry, The Affiliated Stomatology Hospital, Chongqing Medical University, Chongqing, China.
[3]Chongqing Municipal Key Laboratory of Oral Biomedical Engineering of Higher Education, Chongqing, China.
[4]Department of Orthopedic Surgery, The First Affiliated Hospital of Chongqing Medical University, Chongqing, China.
[5]Department of Prosthodontics, The Affiliated Stomatology Hospital, Chongqing Medical University, Chongqing, China.
[6]Molecular Oncology Laboratory, Department of Orthopaedic Surgery and Rehabilitation Medicine, The University of Chicago Medical Center, Chicago, Illinois.
[7]Ministry of Education Key Laboratory of Diagnostic Medicine and School of Laboratory Medicine, Chongqing Medical University, Chongqing, China.
[8]Department of Orthopaedic Surgery, The Second Affiliated Hospital, Chongqing Medical University, Chongqing, China.

[11]. Dentin sialophosphoprotein (Dspp) and dentin matrix protein 1 (Dmp1) are highly expressed in odontoblasts, and they are essential for the development of dentin formation [7,12–14]. Dspp and Dmp1 mutants in both human and mice exhibit abnormal teeth, such as dentinogenesis imperfecta, and dentin hypomineralization [15,16]. As one of the five types of dental stem cells, the stem cells from apical papilla (SCAPs) reside in the apical papilla of immature teeth with an underdeveloped apex. SCAP cells are essential for the development of the tooth, and they can differentiate into odontoblasts for the formation of root dentin [17]. We and others have demonstrated that SCAPs are capable of differentiating into osteo-/odontogenic lineages both in vitro and in vivo [18–20].

Bone morphogenetic proteins (BMPs) belong to the transforming growth factor-β (TGF-β) superfamily and play important roles in bone formation, dental development, and stem cell differentiation [21]. It has been recently demonstrated that BMPs, such as BMP2, BMP4, and BMP7, significantly impact tooth development. BMP2 is considered a contributor to postnatal tooth development and regulates ameloblast and odontoblast differentiation [22,23]. Under the inactivation of BMP4 in the dental mesenchyme, the molar development was affected [24]. The expression of BMP7 was detected in the oral and dental epithelium at the initiation stage of tooth formation, then in odontoblasts and ameloblasts at a later stage [25]. However, little has been reported about possible roles of BMP9 signaling in tooth development. BMP9, also known as growth differentiation factor 2, is a relatively poorly characterized member of the BMP family, which was first isolated from fetal mouse liver cDNA libraries [26]. We previously demonstrated that, among the 14 types of human BMPs, BMP9 is one of the most potent factors that can induce osteogenic differentiation of mesenchymal stem cells (MSCs) both in vivo and in vitro [27,28]. We also found that BMP9 can effectively induce odontoblastic differentiation of SCAP cells and upregulate odontoblastic differentiation markers expression in vitro [18]. Further, we demonstrated that BMP9 acts synergistically with Wnt/β-catenin signaling, another family of critical regulators for tooth development, in promoting odontoblast differentiation of SCAPs [19]. These findings strongly suggest that BMP9 may play an important role in regulating tooth development. Thus, it is critical to investigate the potential functional roles of BMP9 during tooth development.

Materials and Methods

Animals

All animal studies were conducted by following the guidelines approved by the Institutional Animal Care and Use Committee (ACUP#71826). The use and care of animals strictly followed the NIH guidelines stipulated in the approved studies. All mice were housed in groups of 2–4 mice per cage in biosafety barriers with a controlled light cycle and given sterile food and water ad libitum. The light-dark cycle was 1:1 with lights on at 7:00 am. Room temperature was 18°C ± 2°C, and humidity was 55% ± 10%. The animals were euthanized with CO_2 overdose followed by cervical dislocation. Tissues were collected for further micro-computed tomography (micro-CT) and/or histologic analyses. Wild-type mice aged on PN4, PN7, PN11, and PN15 ($n = 3$ each group) were used for detecting the expression pattern of BMP9 in tooth germ during postnatal tooth development. Further, 3-month-old, male *BMP9* null mice and wild-type littermates ($n = 6$ each group) were used for investigating the function of BMP9 in tooth-alveolar bone complex development.

Generation of BMP9 knockout (BMP9-KO) mice

BMP9 null mutants, hereafter referred to as *BMP9*-KO, were generated in The University of Chicago Transgenic Core Facility by using commercially available ES cells with the $GDF2^{tm1}$(from KOMP, Knockout Mouse Project Repository, https://www.komp.org) Vlcg allele (Regeneron) and maintained on C57BL6 background. Wild-type ($BMP9^{+/+}$) and *BMP9*-KO mice for all experimental procedures were produced from $Bmp9^{+/-}$ crosses (Fig. 2A, a).

For genotyping of the mutant mice, the genomic DNA was isolated from mouse tail samples. Specifically, the mouse tail biopsies were incubated in alkaline lysis buffer (0.2 M NaOH, 1 mM EDTA) for 30 min at 85°C. Lysates were diluted 1: 5 in molecular-grade water and used as templates for touchdown polymerase chain reaction. Genotypes were confirmed by using primers targeted for amplification of exon1, exon2, lacz, and neo (Fig. 2A, b). The primer pair (PP) sequences are as follows: PP1, 5′-TGAGTCCCATCTCCATCCTC-3′ and 5′-ATGCAGGACCGTACCAGAAC-3′; PP2, 5′-GGCATCT TGCTCTGAAGGAC-3′ and 5′-GGGCAGTCAGAAAACT CAGC-3′; PP3,5′-CAGTAGTCAGCATCCTTTCC-3′and 5′-GCTGGCTTGGTCTGTCTGTCCTA-3′; and PP4, 5′-GCA GCCTCTGTTCCACATACACTTCA-3′ and 5′-AGTTTCTG CCTGGTTTCCTG-3′.

Hematoxylin and eosin and immunohistochemistry staining

The mandible samples were harvested and fixed in neutral paraformaldehyde solution (Solarbio, Beijing, China) for 2 days, demineralized with EDTA (Biosharp, China) solution, dehydrated through graded alcohol, and finally embedded in paraffin. The embedded samples were serially sectioned, deparaffinized, rehydrated, and subjected to hematoxylin and eosin (H & E; Solarbio, Beijing, China) staining.

The immunohistochemical staining was carried out as previously described [29–31]. Briefly, the slides were blocked and incubated with the primary antibody (Polyclonal rabbit anti-BMP9, 1:100; Thermo Fisher, U.S.; no.PA5-11931) at 4°C overnight. After being washed, the slides were incubated with secondary antibody kit (ZSGB, China; PV-9001) according to the manufacturer's instructions, followed by incubation with diaminobenzidine (Sigma-Aldrich, St. Louis, MO). Cell nuclei were counterstained with hematoxylin. The staining results were photographed under a bright-field microscope (Leica, Germany). Non-immune serum was used as a negative control for mouse primary antibodies.

Micro-CT analysis

Mandibles and maxillae were harvested from 3-month-old *BMP9-KO* and wild-type mice, fixed in neutral paraformaldehyde solution (Solarbio, Beijing, China) for 2 days,

and scanned with micro-CT (Viva CT 40; Scanco Medical, Bassersdorf, Switzerland) at 70 kVp, 114 uA with a 15-μm voxel size. Three-dimensional (3-D) images were analyzed by Image Processing Language to evaluate the tooth and bone volumes.

Digital images were acquired from micro-CT imaging and were analyzed by measuring root length, root dentin thickness, the height of alveolar ridge, trabecular thickness (Tb.Th.), bone volume fraction (BV/TV), and bone mineral density (BMD) by using the micro-CT V6.1 software. The distance from the amelocemental junction to the top of the mesial root was representative of the root length; the thickness of dentin at the middle of the root was representative of the thickness of radicular dentin; and the distance from the top of the inter-alveolar to the link of the mesial and distal root tops represented the height of the alveolar ridge. To obtain Tb.Th., BV/TV, and BMD, the area between the mesial and distal root of the first molar was measured volumetrically through 10 serial sections (150 μm span). Specially, contour lines were drawn between the mesial and distal root of the first molar to define the alveolar bone region of interest (ROI) in micro-CT 2D sagittal sections. Once the 10 serial sections were defined, the sections were submitted for reconstructing the ROI. Finally, the structural parameters (Tb.Th, BV/TV, and BMD) of the reconstructed ROI were calculated. In addition, the mineral density of the enamel and dentin of the first molar was determined by the same method.

3-D reconstruction analysis of the tooth

The teeth of mice were reconstructed by importing the micro-CT DICOM dataset into Mimics 17.0 (Materialise NV, Leuven, Belgium) system. The distance from the amelocemental junction to the top of the mesial root was chosen for measuring the length of the root. The width of the apical foramen was determined in the mesial root in buccolingual directions. In *BMP9*-KO mice and wild-type mice, sections at the 1/2 length of the mesial root were selected to measure the thickness of radicular dentin.

Cell culture, recombinant adenoviruses

The immortalized mouse dental apical papilla (iSCAPs) were previously characterized [18]. The 293 pTP line was used for adenovirus amplification [32]. Both iSCAP and 293pTP cells were maintained in complete Dulbecco's modified Eagle's medium (Sigma-Aldrich, St. Louis, MO) containing 10% fetal bovine serum (GIBCO, CA), 100 units of penicillin (Sigma-Aldrich), and 100 μg of streptomycin (Sigma-Aldrich) at 37°C in 5% CO_2. Recombinant adenoviruses overexpressing BMP9, green fluorescent protein (GFP), or silencing expressing BMP9 (siBMP9) were constructed as previously reported [33]. Polybrene (10 μg/mL; Sigma-Aldrich) was used to enhance transduction efficiency for adenoviral infection [34].

Alkaline phosphatase histochemical staining and quantification assays

The iSCAPs were seeded in 24-well plates and infected with indicated multiplicty of infection (MOI) values of AdGFP, AdBMP9, or AdsiBMP9. Polybrene (10 μg/mL) was used to enhance transduction efficiency for adenoviral infection. At 48 h after the infection, GFP signal or red fluorescent protein (RFP) signal of the infected iSCAPs was assessed under a fluorescence microscope (Carl Zeiss Microimaging GmbH, Gottingen, Germany). The infection efficiency was indicated by the GFP or RFP expression proportion of the cells. Alkaline phosphatase (ALP) histochemical staining was carried out by using the NBT/BCIP staining kit (Beyotime-Bio, China), and ALP activity was assessed quantitatively with the ALP assay kit (Beyotime-Bio, China) on day 5. Each assay condition was performed in triplicate, and the results were repeated in at least three independent experiments. ALP activity was normalized by total cellular protein concentrations determined by the bicinchoninic acid Protein Assay Kit (Beyotime-Bio, China).

RNA isolation, reverse transcription, and quantitative real-time PCR

Total RNA was isolated by using the Trizol reagent (Takara, Japan), and it was subjected to reverse transcription by using the cDNA Reverse Transcription Kit (Takara, Japan). The quantitative real-time PCR analyses were carried out in the ABI Prism 7,500 Real-Time PCR System (Applied Biosystems, Foster City, CA) with the SYBR Green PCR master mix reagent (Takara, Japan). Briefly, the quantitative real-time PCR reaction cycling program was 94°C for 2 min 30 s for 1 cycle; 94°C for 25 s, 65°C for 30 s, and 72°C for 40 s for 10 cycles decreasing 1°C per cycle; and finally, 94°C for 25 s, 60°C for 30 s, 72°C for 40 s for 24 cycles, and 72°C for 10 min. PCR primer sequences were as follows: for mouse *Gapdh*, 5′-ACCCAGAAGACTGTG GATGG-3′ and 5′-CACATTGGGGGTAGGAACAC-3′; for mouse *Dmp1*, 5′-CAGTGAGGATGAGGCAGACA-3′ and 5′-TCGATCGCTCCTGGTACT CT-3′; for mouse *Dspp*, 5′-GGAACTGCAGCACAGAATGA-3′ and 5′-CAGTGTTCC CCT GTTCGTTT-3; and for mouse *BMP9*, 5′-TGAGTCCC ATCTCCATCCTC-3′ and 5′-ACCCACCAGACACAAG AAGG-3′. The $2^{-\Delta\Delta Ct}$ value was used to calculate the relative gene expression normalized by the expression level of Gapdh.

Statistical analysis

Data were expressed as mean ± standard deviation. Statistical significances were determined by the Student's *t*-test or one-way analysis of variance with the use of SPSS 17.0 (SPSS, Inc., Chicago, IL). The differences between groups were statistically significant at $*P < 0.05$.

Results

Expression pattern of BMP9 during postnatal tooth development

Tooth development included two parts: crown development and root development. Generally, the crown continues to develop until PN4; the root starts to develop after crown formation and reaches its final length; and the molar erupts to the oral cavity about PN18 in the mice [35]. In this study, the result of H & E staining demonstrated that at the time of PN4 (Fig. 1A, A′), the crown of the first mandibular molar developed to its final morphology. At PN7, the Hertwig's Epithelial Root Sheath formed (Fig. 1B, B′). The root

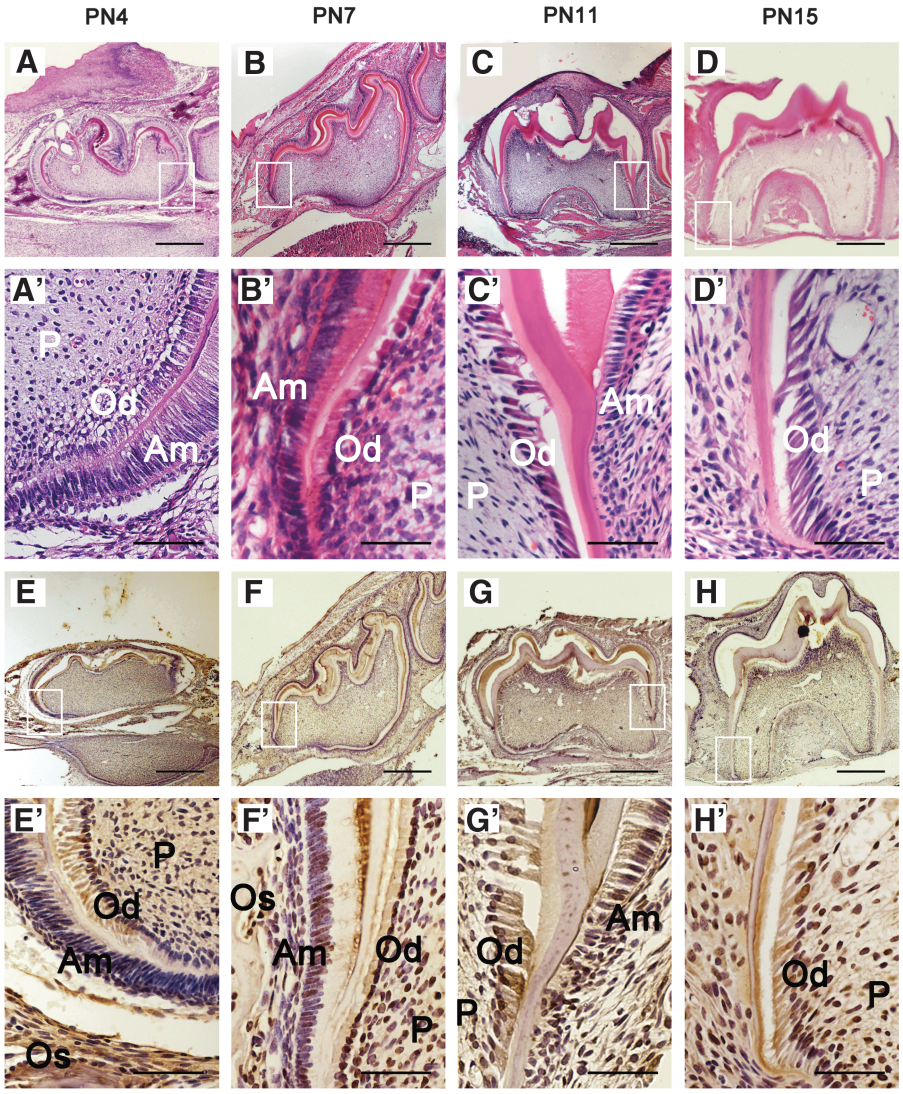

FIG. 1. Expression pattern of BMP9 in tooth germ during postnatal tooth development. **(A–D)** H & E staining of the first mandibular molar in mice at PN4, PN7, PN11, and PN15. **(A′–D′)** Magnification of **(A–D)**. **(E–H)** BMP9 expression in the first molar of mice at PN4, PN7, PN11, and PN15 by immunohistochemistry. **(E′–H′)** Magnification of E-H. BMP9 expression was observed in odontoblasts, ameloblasts, dental pulp, and osteoblasts. Od, odontoblasts; Am, ameloblasts; P, dental pulp; Os, osteoblasts. Scale bars: 500 or 50 μm. H & E, hematoxylin and eosin; BMP, bone morphogenetic protein. Color images are available online.

fraction appeared at PN11 (Fig. 1C, C′), and the root length continued to elongate through PN15 (Fig. 1D, D′). According to the findings, we selected PN4 as the time point for crown development; PN7, PN11, and PN15 as the time points of the initiation, early, and late stages of root development in our subsequent study. To determine whether BMP9 is expressed during postnatal crown and root development, we detected the BMP9 signal in the first mandibular molar by immunohistochemistry at PN4, 7, 11, and 15. On PN4 (Fig. 1E, E′), BMP9 expression was widely observed in odontoblasts, ameloblasts, dental pulp cells, and osteoblasts in alveolar bones. The expression patterns of BMP9 on days PN7 (Fig. 1F, F′), PN11 (Fig. 1G, G′), and PN 15 (Fig. 1H, H′) were similar to PN4. The findings indicate that BMP9 may play a role in postnatal tooth development.

Macrographic morphology of the tooth in BMP9-KO mice

To investigate the function of BMP9 in tooth-alveolar bone complex, we established a *BMP9*-KO mice model. The *BMP9* knockout mice were established and appropriately genotyped as shown in Figure 2A. The *BMP9*-KO mice were viable and fertile, and they did not display gross anatomical abnormalities. Although the detailed analyses of possible phenotypes in different tissues/organs are underway, this study focused on the effect of *BMP9* deficiency on tooth development. To simplify the experimental process, we used a cohort of 3-month-old male *BMP9*-KO mice and their wild-type littermates for this study.

Macrographically, the *BMP9*-KO mice displayed an abnormal tooth phenotype. Specifically, the incisor tips of the *BMP9*-KO mice were abraded, compared with those of the wild-type mice (Fig. 2B). The extracted molars of *BMP9*-OK mice were smaller with flatter cusps and shorter roots, whereas the tooth cusps of the wild-type mice were sharp with longer roots (Fig. 2C). These results suggest that BMP9 deficiency may negatively impact the mouse incisor and molar tooth development.

Micro-CT analysis of tooth-alveolar bone complex structure in BMP9-KO mice

Quantitative high-resolution analysis of the micro-CT image data further demonstrated that *BMP9*-KO mice had a shorter root, bigger apical foramen, and a lower alveolar

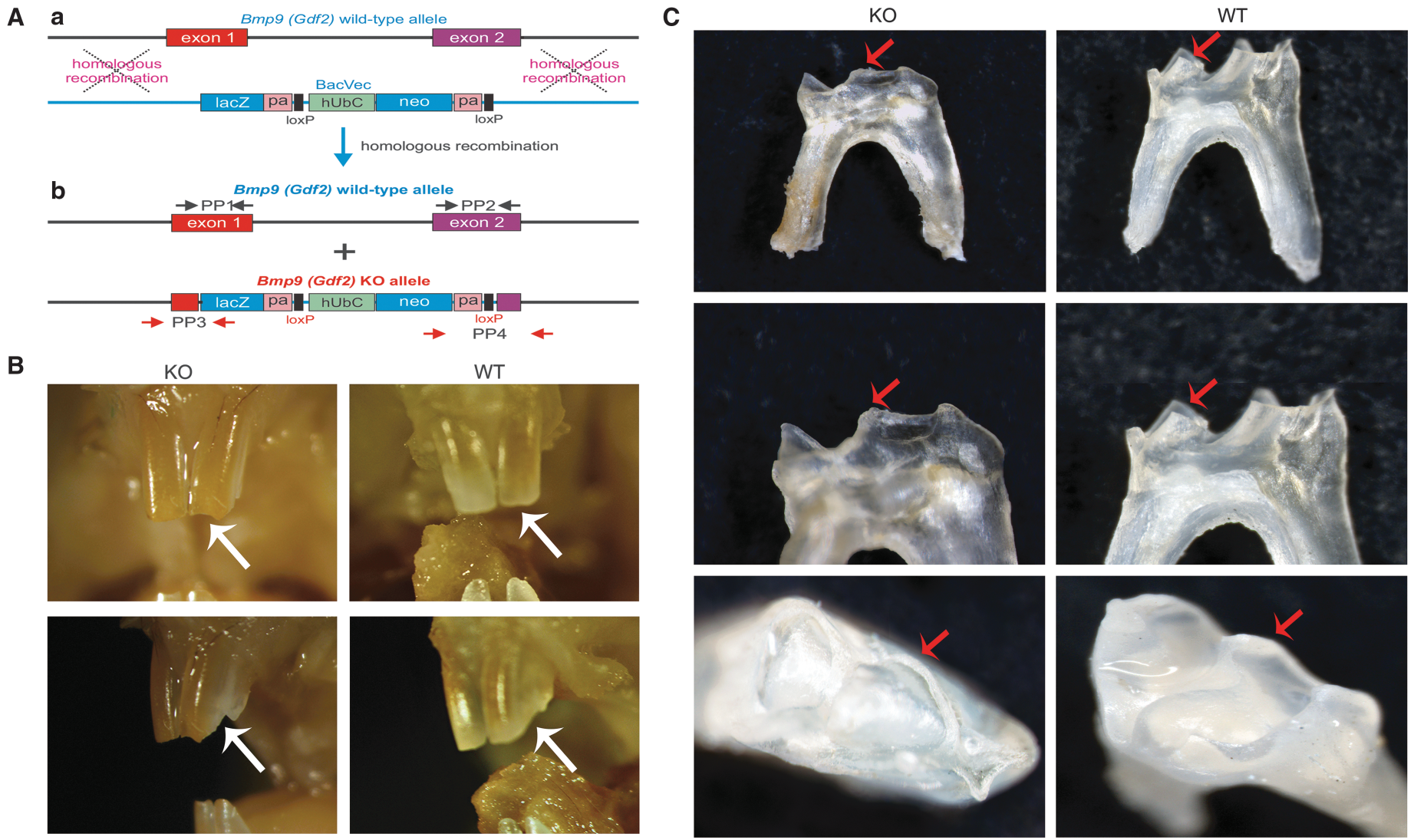

FIG. 2. Gross morphology of teeth in the *BMP9*-KO mice. **(A)** Gene targeting strategy for generating *BMP9*-KO mice**. (a)** *BMP9* null mutants, hereafter referred to as *BMP9*-KO, were generated in The University of Chicago Transgenic Core Facility by using commercially available ES cells with the $Gdf2^{tm1}$ (KOMP) Vlcg allele (Regeneron). Wild-type ($BMP9^{+/+}$) and *BMP9*-KO ($BMP9^{-/-}$) mice for all experimental procedures were produced from **(b)** subsequently derived $BMP9^{\pm}$. Wild-type and *BMP9*-KO mice were identified by using genotyping primers for exon 1 (PP1), exon 2 (PP2), lacZ (PP3), and neo (PP4). PP, primer pair. **(B)** Representative images of tooth morphology of the *BMP9*-KO and wild-type mice. The incisor tip was worn in *BMP9*-KO mice, which was intact in wild-type control (*white arrows*). **(C)** The first mandibular molar from *BMP9*-KO mutants versus wild-type littermates. The *BMP9*-KO mice displayed smaller molars with shorter roots and obvious worn cusps compared with wild-type mice. *Red arrows* indicated the molar cusps. Color images are available online.

ridge, compared with those of the wild-type animals (Fig. 3A). Moreover, the root canal of the first molar from *BMP9*-KO mice was significantly enlarged whereas the dentin wall was thinner (Fig. 3A). Figure 3B demonstrated the method to measure the structural parameters of tooth and alveolar bone listed in C–I. Statistical analysis revealed that the root length and dentin thickness of the *BMP9*-KO group were significantly reduced (Fig. 3C, D). The *BMP9*-KO mice exhibited a marked decrease in alveolar ridge height (Fig. 3E), Tb.Th. (Fig. 3F), BV/TV (Fig. 3G), and the average BMD (Fig. 3H) of alveolar bone. Further, the mineral densities of the enamel and dentin in the *BMP9*-KO mice were significantly lower than those of the wild-type mice (Fig. 3I). Thus, these results suggest that BMP9 deficiency may inhibit the normal development and/or growth of the tooth-alveolar complex.

Tooth abnormalities in BMP9-KO mice determined by 3-D reconstruction mimics analysis

We further carried out the 3-D reconstruction analysis to model tooth abnormalities in the absence of BMP9.

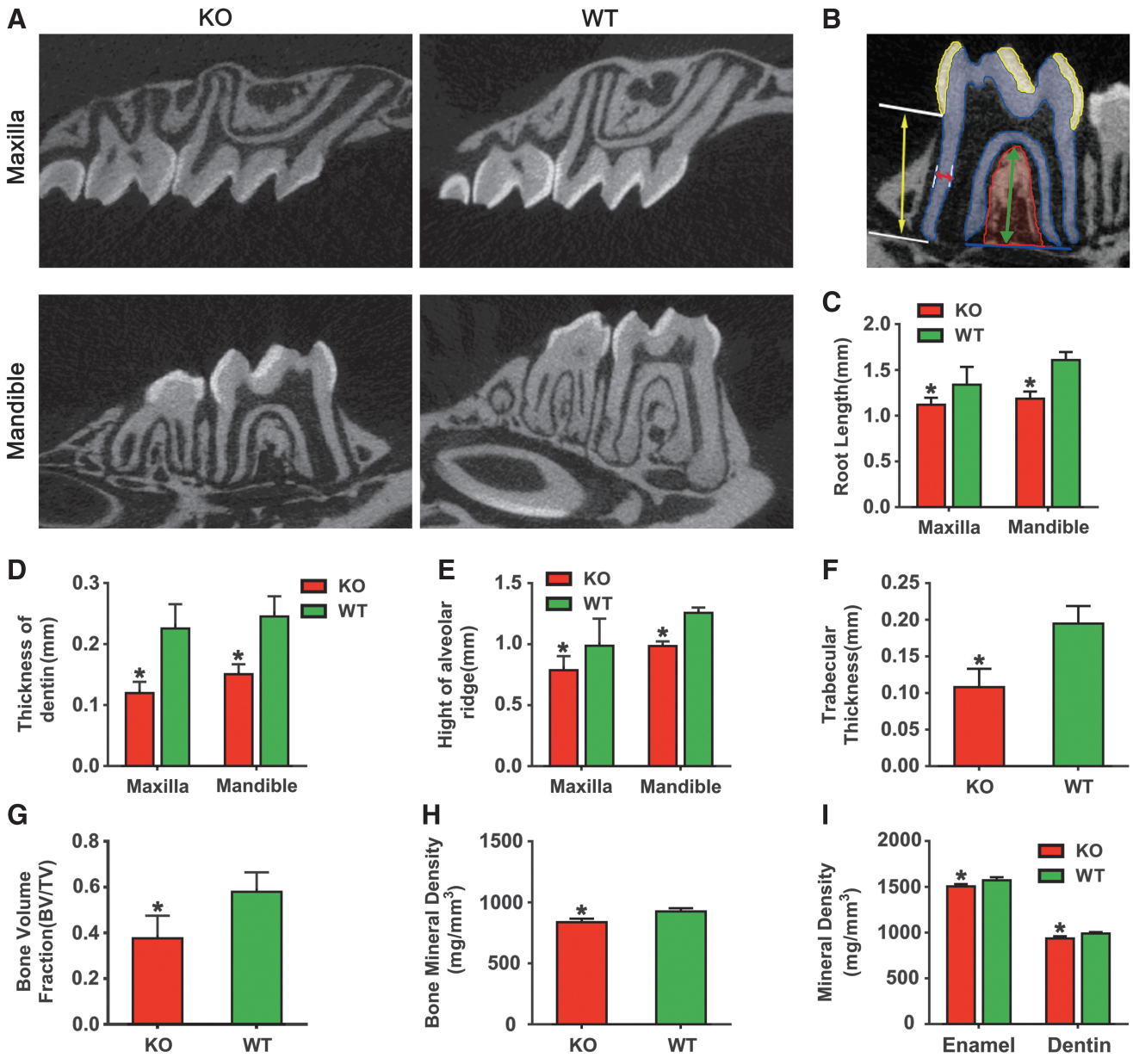

FIG. 3. Micro-CT analysis of the tooth-alveolar bone complex of *BMP9*-KO mice. **(A)** Representative images of the first molar. **(B)** The representative image of the methods used to quantitatively measure the parameters listed in **(C–I)**. *Yellow arrows* indicated root length, *red* indicated dentin thickness, and *green* indicated height of alveolar ridge. The area *highlighted* in *red* marked the alveolar bone ROI, the *yellow* area marked the enamel ROI, and the *blue* area marked the dentin ROI. Quantitative analysis of **(C)** root length, **(D)** dentin thickness, **(E)** height of alveolar ridge, **(F)** trabecular thickness, **(G)** BV/TV, **(H)** bone mineral density of alveolar bone, and **(I)** enamel and dentin mineral density. Data were presented as mean ± standard deviation (SD); $*P < 0.05$, when compared with those of the wild-type littermates. ROI, region of interest; Micro-CT, micro-computed tomography; BV/TV, bone volume fraction. Color images are available online.

Representative 3-D reconstruction images revealed that the first molar of *BMP9*-KO mice had a shorter root, bigger apical foramen, and thinner dentin compared with the wild-type in both maxilla and mandible (Fig. 4A, B). Moreover, the incisor tips of *BMP9*-KO mice were defective and dental pulp chambers were exposed, which were intact without any exposed pulp chambers in the wild-type incisors (Fig. 4C). When the root length and apical foramen width were determined, the root length was significantly decreased (Fig. 4D), whereas apical foramen width was increased in the *BMP9*-KO group (Fig. 4E). Quantitative analysis further revealed that dentin thickness was significantly decreased in the *BMP9*-KO group (Fig. 4F). Thus, this 3-D reconstruction mimics analysis further confirms that the deletion of BMP9 may significantly inhibit the normal development of the tooth.

H & E and immunohistochemical staining of teeth in BMP9-KO mice

Histological stains confirmed the lack of BMP9, resulting in significant tooth abnormalities in the tooth tissues retrieved from *BMP9*-KO mice (Fig. 5A, B). Specifically, H & E staining revealed that the odontoblasts were abundantly

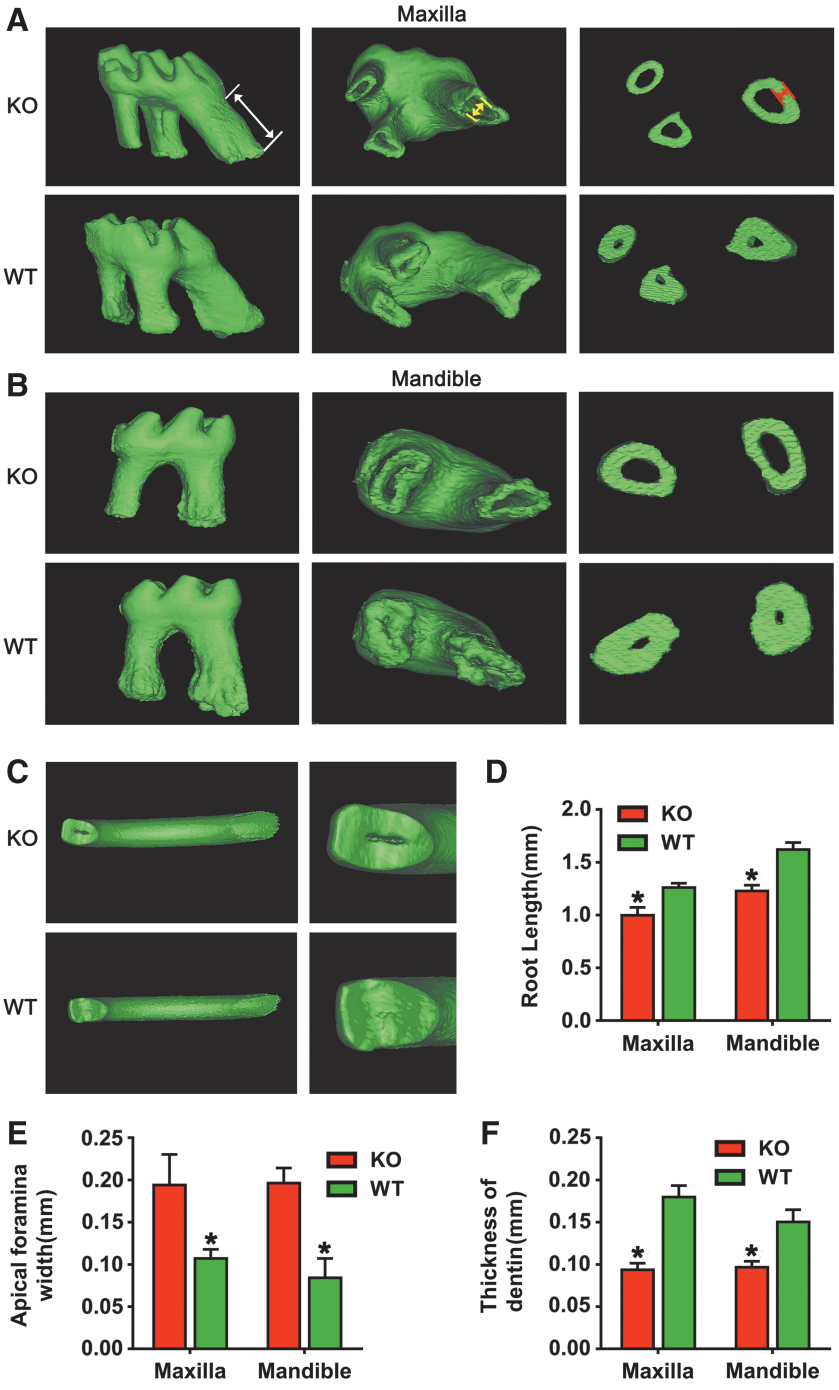

FIG. 4. 3-D reconstruction analysis of the tooth of *BMP9*-KO mice. **(A, B)** The first molar in maxilla and mandible and the cross-section at the middle of the root from *BMP9*-KO and wild-type mice were subjected to 3-D reconstruction analysis. *White arrow* indicated root length, *yellow* indicated apical foramen width, and *red* indicated dentin thickness. **(C)** The incisor tips of *BMP9*-KO mice versus wild-type control mice. **(D–F)** Quantitative analysis of **(D)** root length, **(E)** apical foramen width, and **(F)** the thickness of root dentin. Data were presented as mean ± standard deviation (SD); $^*P < 0.05$, when compared with those of the wild-type littermates; 3-D, three-dimensional. Color images are available online.

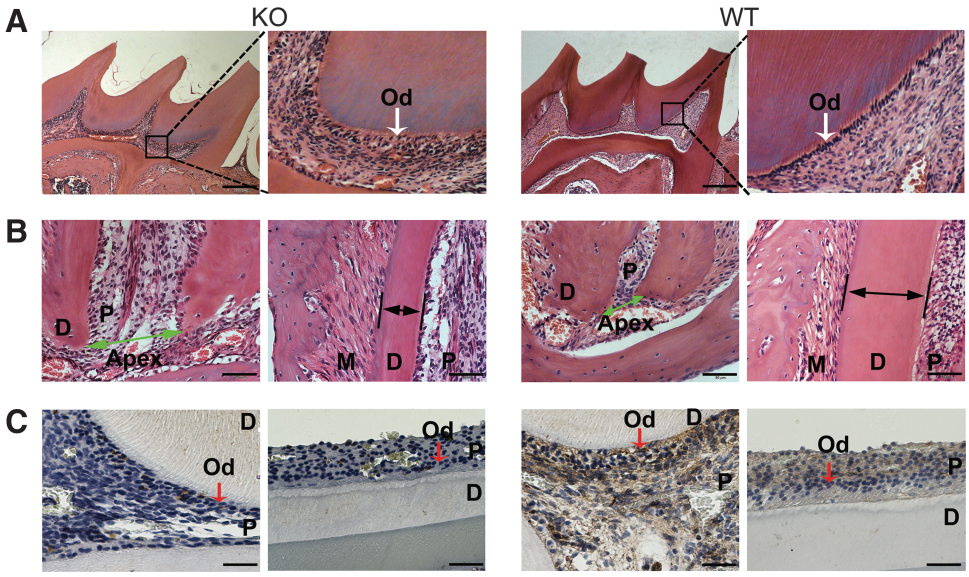

FIG. 5. H & E and immunohistochemical staining of tooth in *BMP9*-KO mice. **(A, B)** H & E staining of tooth samples retrieved from the *BMP9*-KO and the wild-type mice. **(A)** The Od were shown (*white arrows*). **(B)** *BMP9*-KO mice showed enlarged apical foramen (*green arrows*) whereas they exhibited reduced thickness of dentin (*black arrows*) compared with wild-type. **(C)** Immunohistochemical detection of BMP9 expression in tooth samples retrieved from the *BMP9*-KO and the wild-type mice. The odontoblasts are indicated by *red arrows*. Od, odontoblasts; P, dental pulp; D, dentin; M, periodontal membrane. Scale bars: 200, 50, or 25 μm. Color images are available online.

presented in polarized and well-organized single layers of cells in the wild-type mice, which was disorganized and formed multiple layers in the *BMP9*-KO mice (Fig. 5A). Further, *BMP9*-KO mice exhibited an enlarged pulp canal and apical foramen with thinner root dentin, compared with those of the wild-type control group (Fig. 5B).

For immunohistochemical staining, there were almost no positively stained cells in the *BMP9*-KO mice tooth, whereas the BMP9 expression was detected in odontoblasts and dental pulp cells in wild-type mice (Fig. 5C), confirming that BMP9 was effectively deleted in the *BMP9*-KO mice.

Silencing BMP9 expression decreases osteo-/odontoblastic marker expression in dental progenitor cells

To further explore how BMP9 regulates osteo-/odontogenic differentiation of dental stem cells, we transduced the iSCAP cells with adenovirus overexpressing BMP9 or expressing siRNAs that silence mouse BMP9 expression. The iSCAPs infected with adenovirus expressing only GFP (AdGFP) were used as controls. The transduction efficiency was indicated by the GFP or RFP expression proportion of the cells, and it was improved with the increasing MOIs of AdBMP9 or AdsiBMP9 at 48 h after infection (Fig. 6A). When iSCAP cells were infected with increasing MOIs of AdBMP9, there was a trend of increasing ALP activity at day 5, whereas ALP activity was decreased when iSCAP cells were infected by increasing MOIs of AdsiBMP9 compared with controls (Fig. 6B, C). Further, the odontogenic markers in iSCAPs, Dmp1 and Dspp, were decreased by silencing the BMP9 expression, whereas they increased when the BMP9 was overexpressed compared with the AdGFP-infected iSCAPs control group (Fig. 6D). Thus, these results strongly suggest that BMP9 may play an important role in regulating the osteo-/odotoblastic differentiation of dental stem cells, such as iSCAPs, and thus may contribute to the normal developmental process of the teeth.

Discussion

In this study, we established the *BMP9*-knockout mouse model and analyzed the role of BMP9 in tooth-alveolar bone complex development. We found that *BMP9*-KO mice showed apparent defects in the tooth-alveolar bone complex, similar to the phenotypes manifested by dentinogenesis imperfecta. Further, we demonstrated that silencing BMP9 expression in iSCAP cells led to decreased expression of odontogenic differentiation makers, Dspp and Dmp1. Taken together, our results strongly suggest that BMP9 may play an important role in regulating tooth development. The novel finding may trigger future studies that are devoted to exploring how BMP9 functions in tooth development and the therapeutic uses of BMP9 for the bioengineering of replacement teeth.

BMP9 is a multiple-functional growth and differentiation factor and it plays a critical role in bone development [36]. Both dentin and bone are mineralized tissues, and they share many similarities in their biochemical properties and biomechanical compositions [37]. However, the role of BMP9 in dentinogenesis and tooth-alveolar bone complex formation is unclear. In an attempt to clarify the role of BMP9 in tooth development, we detected the BMP9 expression in tooth germs. According to the results of immunohistochemical staining, the expression of BMP9 was observed in odontoblasts, ameloblasts besides its expression in dental pulp and osteoblasts in alveolar bone during postnatal tooth development. The wide and intensive expression of BMP9 in the tooth germ suggests that BMP9 plays an important role in tooth development. Although some other BMP

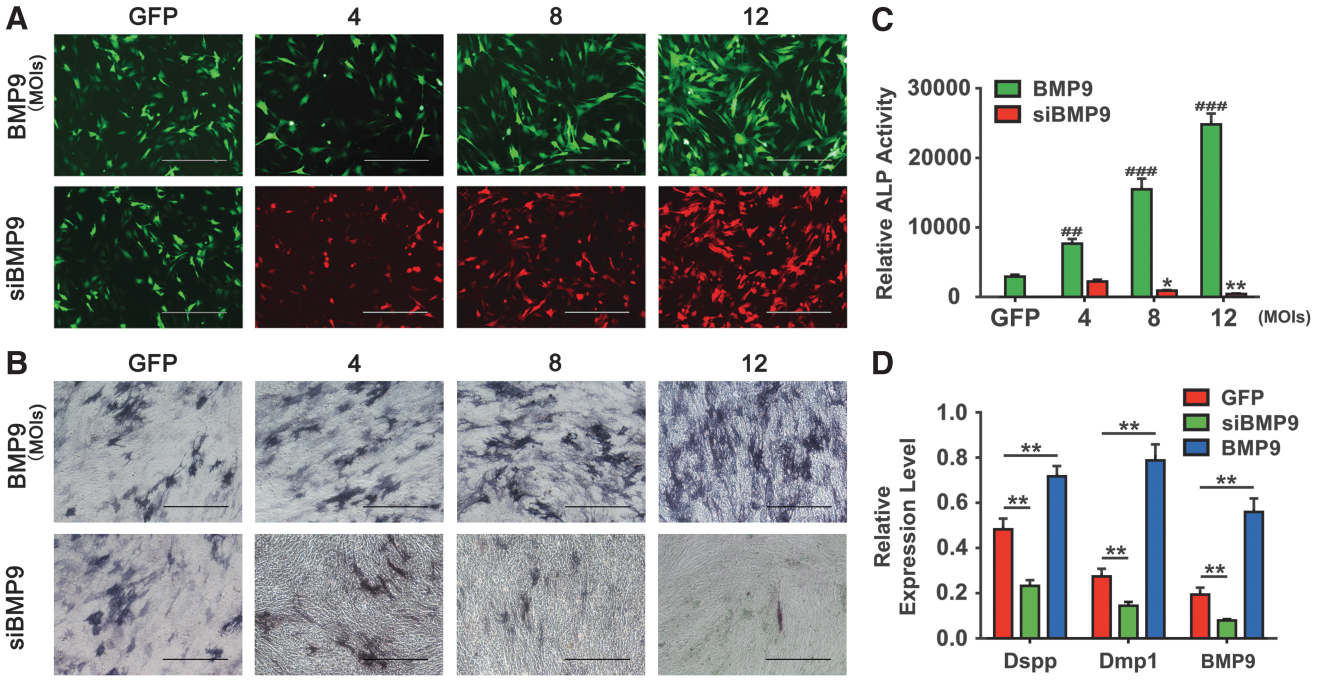

FIG. 6. Silencing BMP9 expression decreases osteo-/odontoblastic marker expression in dental progenitor cells. **(A)** The GFP and RFP expression of the infected iSCAPs improved with the increased MOIs of AdBMP9 or AdsiBMP9 at 48 h after infection. The infection efficiency was indicated by the GFP or RFP expression proportion of the cells. **(B)** ALP histochemical staining assay. Subconfluent iSCAP cells were infected with the indicated MOIs of AdGFP, AdBMP9, or AdsiBMP9. At 5 days after infection, ALP staining assays were carried out. Representative staining results are shown. Scale bars: 400 μm. **(C)** Quantitative ALP assay. The iSCAPs were seeded in 24-well plates, and the treatment conditions were the same as those described in **(B)**. #Indicated the significance between BMP9 and GFP control group, $\#\#P < 0.01$; $\#\#\#P < 0.001$; *shows the significance between siBMP9 and GFP control group, $*P < 0.05$; $**P < 0.01$. **(D)** Relative mRNA expression of Dspp, Dmp1, and BMP9 was determined by qPCR. Subconfluent iSCAP cells were infected with AdGFP, AdsiBMP9, or AdBMP9 for 5 days. Total RNA was isolated and subjected to reverse transcription and quantitative real-time PCR by using primers specific for mouse Dspp, Dmp1, BMP9, as well as Gapdh. The $2^{-\Delta\Delta Ct}$ value was used to calculate the relative gene expression normalized by the expression level of Gapdh. Each assay condition was done in triplicate. $**P < 0.01$ compared with the AdGFP-infected iSCAPs control group. GFP, green fluorescent protein; RFP, red fluorescent protein; ALP, alkaline phosphatase; Dspp, dentin sialophosphoprotein; Dmp1, dentin matrix protein 1; iSCAP, immortalized mouse dental apical papilla. MOIs, multiplicities of infection; qPCR, quantitative real-time PCR. Color images are available online.

molecules, including BMP2, BMP4, and BMP7, were also detected in odontoblasts and ameloblasts during the dentinogenesis and amelogenesis [24,38,39], the defects in the tooth of *BMP9*-KO mice suggest that the absence of BMP9 cannot be compensated by other BMP molecules.

Dentinogenesis imperfect III (DI-III) is a genetic disease in humans that is characterized by severe dentin hypomineralization, thinner and shorter roots, and pulp enlargement occurring during the tooth development [40–42]. In our study, micro-CT and 3-D reconstruction analysis of the *BMP9* mutant mouse tooth displayed reduced thickness dentin, enlarged pulp canals, and shortened roots. These characteristics of *BMP9*-KO mice are similar to those of DI-III. To date, several studies have reported that molecular regulation is necessary for dentinogenesis and the root development.

Dspp is the terminal differentiation marker of odontoblasts and is abundant in the dentin matrix. The predentin in the *Dspp* gene deletion mouse is hypomineralized, similar to human dentinogenesis imperfecta Type III [43]. *Dspp* null mice exhibit impaired tooth and alveolar bone development that persist through postnatal growth, including remarkable alveolar bone loss, lower BV/TV and mineral density, and irregular tooth root [44–46]. These changes in dentin and alveolar bone found in the *Dspp* null mice are similar to those observed in our *BMP9*-KO mutations. Dmp1 is a key regulator of odontoblast differentiation, and the expression of Dmp1 is required in both early and late odontoblasts for normal odontogenesis and mineralization [13,47]. *Dmp1* gene loss mice exhibit expansion of the pulp cavities and root canals and thin dentin [15,48], which had some similarities to the manifestations of *BMP9*-KO mice. The re-expression of Dmp1 in odontoblasts rescued the defects of dentin mineralization in *Dmp1* null mice [47]. As shown in our studies, both Dspp and Dmp1 were significantly induced by BMP9, whereas their expression was reduced when BMP9 was silenced, suggesting that both Dspp and Dmp1 may be critical downstream targets of BMP9 signaling in dental development. Nonetheless, it remains to be determined clinically whether the lack of or decreased BMP9 expression is associated with the development of dentinogenesis imperfecta.

Teeth are stabilized on the alveolar bone by periodontal ligament, and the well-developed alveolar bone is important

for tooth function. It was reported that appropriate subcrestal BMD and height of the alveolar bone and the alveolar ridge are important for supporting the tooth [49]. In our study, we found BMP9 expression in alveolar bone during the stages of tooth germ, suggesting that BMP9 may play a part in alveolar bone development. Further, we found that the adult *BMP9*-KO mice had a shorter alveolar bone and decreased mineral density, Tb.Th. and BV/TV, compared with the wild-type control mice. A previous study proved that the source of alveolar bone is a part from the dental follicle mesenchymal cells that differentiate into osteoblasts [50]. We and others demonstrated that BMP9 can effectively induce osteogenic differentiation and bone regeneration of dental stem cells and MSCs by altering the expression of key regulators of osteogenesis, both in vivo and in vitro [18,51,52]. Further, silencing the expression of BMP9 can diminish the osteogenic differentiation, matrix mineralization, and ectopic bone formation from MSCs [33]. In our study, we found that silencing the expression of BMP9 in iSCAPs effectively inhibited the expression of osteogenic differentiation maker, ALP. These findings suggest that the defective alveolar bone in BMP9-KO mice may result from the inhibition of osteogenic differentiation by BMP9 deficiency. However, future studies should be directed toward investigating the detailed regulatory circuitry of BMP9 signaling in dentinogenesis and tooth-alveolar bone development.

Conclusions

In this study, *BMP9*-KO mice displayed defects in the tooth-alveolar bone complex. The *BMP9* null mice demonstrated thinner dentin, shorter roots, and enlarged root pulp canals that resemble the manifestations of DI-III. Moreover, the alveolar bone in *BMP9-KO* mice was shorter and hypomineralization was observed. Mechanistically, we found that the expression of Dspp and Dmp1 was inhibited when BMP9 was silenced in iSCAPS, suggesting that Dspp and Dmp1 may be critical downstream targets of BMP9 signaling in dental development. Nonetheless, further studies are required to determine whether the lack of or decreased BMP9 expression is associated with the development of dentinogenesis imperfecta clinically.

Acknowledgments

The reported work was supported in part by research grants from the National Natural Science Foundation of China (#81870758 to HZ), Chongqing Research Program of Basic Research and Frontier Technology (#cstc2017jcyjAX0020 to HZ), the Program for Innovation Team Building at Institutions of Higher Education in Chongqing in 2016 (#CXTDG201602006), the National Institutes of Health (CA226303 to TCH), and the National Key Research and Development Program of China (2016YFC1000803 and 2011CB707906). TCH was also supported by the Mabel Green Myers Research Endowment Fund and The University of Chicago Orthopaedic Surgery Alumni Fund. Funding sources were not involved in the study design; in the collection, analysis, and interpretation of data; in the writing of the article; and in the decision to submit the article for publication.

Author Disclosure Statement

No competing financial interests exist.

References

1. Hasegawa K, H Wada, K Nagata, H Fujiwara, N Wada, H Someya, Y Mikami, H Sakai and T Kiyoshima. (2016). Facioscapulohumeral muscular dystrophy (FSHD) region gene 1 (FRG1) expression and possible function in mouse tooth germ development. J Mol Histol 47:375–387.
2. Lee HK, JW Park, YM Seo, HH Kim, G Lee, HS Bae and JC Park. (2016). Odontoblastic inductive potential of epithelial cells derived from human deciduous dental pulp. J Mol Histol 47:345–351.
3. Guobin Y, Y Guohua, Y Wenduo, KWY Cho and C Yiping. (2014). An atypical canonical bone morphogenetic protein (BMP) signaling pathway regulates Msh homeobox 1 (Msx1) expression during odontogenesis. J Biol Chem 289:31492–31502.
4. Lu L, L Minkui, W Ying, C Peter, C Zhi and C Yiping. (2011). BmprIa is required in mesenchymal tissue and has limited redundant function with BmprIb in tooth and palate development. Dev Biol 349:451–461.
5. Young-Man L, S Seung-Yun, J Seong-Suk, K Il-Keun, C Eun-Hee, C Eui-Sic, P Sang-Hyuk and K Eun-Cheol. (2014). The role of PIN1 on odontogenic and adipogenic differentiation in human dental pulp stem cells. Stem Cells Dev 23:618–630.
6. Fan L, S Deng, X Sui, M Liu, S Cheng, Y Wang, Y Gao, CH Chu and Q Zhang. (2018). Constitutive activation of β-catenin in ameloblasts leads to incisor enamel hypomineralization. J Mol Histol 49:499–507.
7. Zhang H, X Xie, P Liu, T Liang, Y Lu and C Qin. (2018). Transgenic expression of dentin phosphoprotein (DPP) partially rescued the dentin defects of DSPP-null mice. PLoS One 13:e0195854.
8. Bronckers ALJJ, G Nur, LlR Renate, S Janna, AP Moraru, H Nina, TJ Bervoets, F Regina, E Vincent and S Paul. (2013). The intramembrane protease SPPL2A is critical for tooth enamel formation. J Bone Miner Res 28:1622–1630.
9. Bae CH, JY Lee, TH Kim, JA Baek, JC Lee, X Yang, MM Taketo, R Jiang and ES Cho. (2013). Excessive Wnt/beta-catenin signaling disturbs tooth-root formation. J Periodontal Res 48:405–410.
10. Li J, X Huang, X Xu, J Mayo, P Bringas, Jr., R Jiang, S Wang and Y Chai. (2011). SMAD4-mediated WNT signaling controls the fate of cranial neural crest cells during tooth morphogenesis. Development 138:1977–1989.
11. Bartlett JD. (2013). Dental enamel development: proteinases and their enamel matrix substrates. ISRN Dent 2013: 684607.
12. Dobrawa N, S Yao, M Izabela, TK Bertin, D Brian, DS Rena, Q Chunlin and L Brendan. (2012). Transcriptional repression of the Dspp gene leads to dentinogenesis imperfecta phenotype in Col1a1-Trps1 transgenic mice. J Bone Miner Res 27:1735–1745.
13. Simon S, AJ Smith, PJ Lumley, A Berdal, G Smith, S Finney and PR Cooper. (2009). Molecular characterization of young and mature odontoblasts. Bone 45:693–703.
14. Guo S, D Lim, Z Dong, TL Saunders, PX Ma, CL Marcelo and HH Ritchie. (2014). Dentin sialophosphoprotein: a regulatory protein for dental pulp stem cell identity and fate. Stem Cells Dev 23:2883–2894.

15. Ling Y, MD Mary, Z Shubin, X Yixia, Z Jianghong, L Zubing, L Yongbo, M Yuji and JQ Feng. (2004). Deletion of dentin matrix protein-1 leads to a partial failure of maturation of predentin into dentin, hypomineralization, and expanded cavities of pulp and root canal during postnatal tooth development. J Biol Chem 279:19141–19148.
16. Porntaveetus T, N Nowwarote, T Osathanon, T Theerapanon, P Pavasant, L Boonprakong, K Sanon, S Srisawasdi, K Suphapeetiporn and V Shotelersuk. (2019). Compromised alveolar bone cells in a patient with dentinogenesis imperfecta caused by DSPP mutation. Clin Oral Investig 23:303–313.
17. Huang TJ, W Sonoyama, L Yi, L He, S Wang and S Shi. (2008). The hidden treasure in apical papilla: the potential role in pulp/dentin regeneration and BioRoot engineering. J Endod 34:645–651.
18. Wang J, H Zhang, W Zhang, E Huang, N Wang, N Wu, S Wen, X Chen, Z Liao, et al. (2014). Bone morphogenetic protein-9 effectively induces osteo/odontoblastic differentiation of the reversibly immortalized stem cells of dental apical papilla. Stem Cells Dev 23:1405–1416.
19. Zhang H, J Wang, F Deng, E Huang, Z Yan, Z Wang, Y Deng, Q Zhang, Z Zhang, et al. (2015). Canonical Wnt signaling acts synergistically on BMP9-induced osteo/odontoblastic differentiation of stem cells of dental apical papilla (SCAPs). Biomaterials 39:145–154.
20. Na S, H Zhang, F Huang, W Wang, Y Ding, D Li and Y Jin. (2016). Regeneration of dental pulp/dentine complex with a three-dimensional and scaffold-free stem-cell sheet-derived pellet. J Tissue Eng Regen Med 10:261–270.
21. Li J, J Feng, Y Liu, TV Ho, W Grimes, HA Ho, S Park, S Wang and Y Chai. (2015). BMP-SHH signaling network controls epithelial stem cell fate via regulation of its niche in the developing tooth. Dev Cell 33:125–135.
22. Miyoshi K, H Nagata, T Horiguchi, K Abe, WI Arie, Y Baba, H Harada and T Noma. (2008). BMP2-induced gene profiling in dental epithelial cell line. J Med Invest 55:216–226.
23. Rakian A, WC Yang, J Gluhak-Heinrich, C Yong, MA Harris, D Villarreal, JQ Feng, M Macdougall and SE Harris. (2013). Bone morphogenetic protein-2 gene controls tooth root development in coordination with formation of the periodontium. Int J Oral Sci 5:75–84.
24. Shihai J, Z Jing, G Yang, B Jin-A, JF Martin, L Yu and J Rulang. (2013). Roles of Bmp4 during tooth morphogenesis and sequential tooth formation. Development 140:423–432.
25. Yamashiro T, M Tummers and I Thesleff. (2003). Expression of bone morphogenetic proteins and Msx genes during root formation. J Dent Res 82:172–176.
26. Song JJ, AJ Celeste, FM Kong, RL Jirtle, V Rosen and RS Thies. (1995). Bone morphogenetic protein-9 binds to liver cells and stimulates proliferation. Endocrinology 136: 4293–4297.
27. Luu HH, S Wen-Xin, L Xiaoji, M David, L Jinyong, D Zhong-Liang, KA Sharff, AG Montag, RC Haydon and H Tong-Chuan. (2010). Distinct roles of bone morphogenetic proteins in osteogenic differentiation of mesenchymal stem cells. J Orthop Res 25:665–677.
28. Kang Q, MH Sun, H Cheng, Y Peng, AG Montag, AT Deyrup, W Jiang, HH Luu, J Luo, et al. (2004). Characterization of the distinct orthotopic bone-forming activity of 14 BMPs using recombinant adenovirus-mediated gene delivery. Gene Ther 11:1312–1320.
29. Ye J, J Wang, Y Zhu, Q Wei, X Wang, J Yang, S Tang, H Liu, J Fan, et al. (2016). A thermoresponsive polydiolcitrate-gelatin scaffold and delivery system mediates effective bone formation from BMP9-transduced mesenchymal stem cells. Biomed Mater 11:025021.
30. Luther GA, J Lamplot, X Chen, R Rames, ER Wagner, X Liu, A Parekh, E Huang, SH Kim, et al. (2013). IGFBP5 domains exert distinct inhibitory effects on the tumorigenicity and metastasis of human osteosarcoma. Cancer Lett 336:222–230.
31. Li R, W Zhang, J Cui, W Shui, L Yin, Y Wang, H Zhang, N Wang, N Wu, et al. (2014). Targeting BMP9-promoted human osteosarcoma growth by inactivation of notch signaling. Curr Cancer Drug Targets 14:274–285.
32. Wu N, H Zhang, F Deng, R Li, W Zhang, X Chen, S Wen, N Wang, J Zhang, et al. (2014). Overexpression of Ad5 precursor terminal protein accelerates recombinant adenovirus packaging and amplification in HEK-293 packaging cells. Gene Ther 21:629–637.
33. Yan S, R Zhang, K Wu, J Cui, S Huang, X Ji, L An, C Yuan, C Gong, et al. (2018). Characterization of the essential role of bone morphogenetic protein 9 (BMP9) in osteogenic differentiation of mesenchymal stem cells (MSCs) through RNA interference. Genes Dis 5:172–184.
34. Zhao C, N Wu, F Deng, H Zhang, N Wang, W Zhang, X Chen, S Wen, J Zhang, et al. (2014). Adenovirus-mediated gene transfer in mesenchymal stem cells can be significantly enhanced by the cationic polymer polybrene. PLoS One 9:e92908.
35. Yang L, F Jifan, L Jingyuan, Z Hu, H Thach-Vu and C Yang. (2015). An Nfic-hedgehog signaling cascade regulates tooth root development. Development 142:3374–3382.
36. Luther G, ER Wagner, G Zhu, Q Kang, Q Luo, J Lamplot, Y Bi, X Luo, J Luo, et al. (2011). BMP-9 induced osteogenic differentiation of mesenchymal stem cells: molecular mechanism and therapeutic potential. Curr Gene Ther 11: 229–240.
37. Kim TH, CH Bae, EH Jang, CY Yoon, Y Bae, SO Ko, MM Taketo and ES Cho. (2012). Col1a1-cre mediated activation of β-catenin leads to aberrant dento-alveolar complex formation. Anat Cell Biol 45:193–202.
38. Feng G, F Junsheng, W Feng, L Wentong, G Qingping, C Zhuo, S Lisa, KJ Donly, GH Jelica and CY Hee Patricia. (2015). Bmp2 deletion causes an amelogenesis imperfecta phenotype via regulating enamel gene expression. J Cell Physiol 230:1871–1882.
39. Xiuqing D, S Bin, R Ningsheng, G Zhen, Z Yanding, C Yiping and H Xuefeng. (2014). Expression patterns of genes critical for BMP signaling pathway in developing human primary tooth germs. Histochem Cell Biol 142:657–665.
40. Dong J, T Gu, L Jeffords and M Macdougall. (2005). Dentin phosphoprotein compound mutation in dentin sialophosphoprotein causes dentinogenesis imperfecta type III. Am J Med Genet A 132:305–309.
41. Cassia A, G Aoun, A Elouta, G Pasquet and R Cavézian. (2017). Prevalence of dentinogenesis imperfecta in a french population. J Int Soc Prev Community Dent 7:116–119.
42. de La Dure-Molla M, B Philippe Fournier and A Berdal. (2015). Isolated dentinogenesis imperfecta and dentin dysplasia: revision of the classification. Eur J Hum Genet 23:445–451.
43. Taduru S, T Tamizchelvi, H Bradford, L Glenn, DS Rena, H Sung, WJ Tim, MD Mary, S John and AB Kulkarni.

(2003). Dentin sialophosphoprotein knockout mouse teeth display widened predentin zone and develop defective dentin mineralization similar to human dentinogenesis imperfecta type III. J Biol Chem 278:24874–24880.
44. Gibson MP, Q Zhu, Q Liu, RN D'Souza, JQ Feng and C Qin. (2013). Loss of dentin sialophosphoprotein leads to periodontal diseases in mice. J Periodontal Res 48:221–227.
45. Gibson MP, P Jani, L Ying, X Wang, Y Lu, JQ Feng and C Qin. (2013). Failure to process dentin sialophosphoprotein (DSPP) into fragments leads to periodontal defects in mice. Eur J Oral Sci 121:545–550.
46. Chen Y, Y Zhang, A Ramachandran and A George. (2016). DSPP is essential for normal development of the dental-craniofacial complex. J Dent Res 95:302–310.
47. Lu Y, Y Ling, S Yu, S Zhang, Y Xie, MD Mckee, CL Yan, J Kong, JD Eick and SL Dallas. (2007). Rescue of odontogenesis in Dmp1-deficient mice by targeted re-expression of DMP1 reveals roles for DMP1 in early odontogenesis and dentin apposition in vivo. Dev Biol 303:191–201.
48. Rangiani A, ZG Cao, Y Liu, AV Rodgers, Y Jiang, CL Qin and JQ Feng. (2012). Dentin matrix protein 1 and phosphate homeostasis are critical for postnatal pulp, dentin and enamel formation. Int J Oral Sci 4:189–195.
49. Johnston BD and WE Ward. (2015). The ovariectomized rat as a model for studying alveolar bone loss in postmenopausal women. Biomed Res Int 2015:635023.
50. Lisa D, M Eva, TA Mitsiadis and AS Tucker. (2010). Contribution of the tooth bud mesenchyme to alveolar bone. J Exp Zool B Mol Dev Evol 312B:510–517.
51. Luo J, M Tang, J Huang, BC He, JL Gao, L Chen, GW Zuo, W Zhang, Q Luo, et al. (2010). TGFbeta/BMP type I receptors ALK1 and ALK2 are essential for BMP9-induced osteogenic signaling in mesenchymal stem cells. J Biol Chem 285:29588–29598.
52. Wu N, Y Zhao, Y Yin, Y Zhang and J Luo. (2010). Identification and analysis of type II TGF-beta receptors in BMP-9-induced osteogenic differentiation of C3H10T1/2 mesenchymal stem cells. Acta Biochim Biophys Sin (Shanghai) 42:699–708.

Address correspondence to:
Dr. Hongmei Zhang
Chongqing Key Laboratory for Oral Diseases and Biomedical Sciences
The Affiliated Hospital of Stomatology
Chongqing Medical University
Chongqing 401147
China

E-mail: drhongmei@sina.com

Dr. Tong-chuan He
Molecular Oncology Laboratory
Department of Orthopaedic Surgery and Rehabilitation Medicine
The University of Chicago Medical Center
5841 South Maryland Avenue, MC 3079
Chicago, IL 60637

E-mail: tche@uchicago.edu

Received for publication November 15, 2018
Accepted after revision February 27, 2019
Prepublished on Liebert Instant Online February 28, 2019